Preparation of Paper (Stage 1): Counting pages and fitting the figures

First A. Author, *Fellow, IEEE*, Second B. Author, and Third C. Author, Jr., *Member, IEEE*

***Abstract*— Distortion-product otoacoustic emissions are intermodulation products upon stimulation by two tones and reflect the nonlinear processing of sound waves within the inner ear by the so-called cochlear amplifier. Therefore, they are interpreted as diagnostic measure of the physiological state of it. Because of their very small amplitudes, current clinical systems measure one distortion product amplitude at typically some 7 frequencies and thus can be regarded as a 1D-Scan. More advanced systems record input-output functions of the distortion product amplitudes, where, however, both tones are varied in a prescribed proportion (2D-scan). When varying both tones independently, a 3D-scan giving a more complete and accurate information about the cochlea under investigation is obtained, but at the cost of vastly extended measurement time. Here, we introduce an adaptive measurement method that is shown to collect more distortion products having sufficient signal-to-noise ratio, and that in the majority of the cases leads to the identification of the so-called individually optimal stimulus level path. We compared the adaptive measurement method to a static one where the stimulus level combination are prescribed beforehand. Within a tolerance of x dB, the adaptive method found the same optimum paths than the static method within the overlap area genertaed by both methods, and added x% more optimum stimulus paths where the static method failed. Ultimately, a bivariate histogram of area and density of the sampling of the optimum path shows that the adaptive method makes a better compromise between two concurring goals, as the compromise achieved is situated closer to the unachievable goal of reaching maximum density and high coverage at the same time. Thus, the adaptive method has been shown to yield a time-efficient approach to characterize the inner ear more comprehensively, which is expected to leads to more accurate diagnosis of the state of the inner ear.**

***Index Terms*— Acoustic distortion, auditory system, biharmonic spline interpolation, distortion measurement, distortion product otoacoustic emissions, Delaunay triangulation, hearing, beta skeleton**

This paragraph of the first footnote will contain the date on which you submitted your paper for review. It will also contain support information, including sponsor and financial support acknowledgment. For example, “This work was supported in part by the U.S. Department of Commerce under Grant BS123456.”

The next few paragraphs should contain the authors’ current affiliations, including current address and e-mail. For example, F. A. Author is with the National Institute of Standards and Technology, Boulder, CO 80305 USA (e-mail: author@boulder.nist.gov).

S. B. Author, Jr., was with Rice University, Houston, TX 77005 USA. He is now with the Department of Physics, Colorado State University, Fort Collins, CO 80523 USA (e-mail: author@lamar.colostate.edu).

T. C. Author is with the Electrical Engineering Department, University of Colorado, Boulder, CO 80309 USA, on leave from the National Research Institute for Metals, Tsukuba, Japan (e-mail: author@nrim.go.jp).

I. Introduction

A. DPOAE, DPOAE Input-output functions and DPOAE level maps for assessment of the cochlear amplifier

Distortion-product otoacoustic emissions (DPOAE) are sound waves generated in the nonlinear, active cochlea through the intermodulation of two-tone stimulation, with stimulus frequencies f_1 and f_2 and their stimulus levels L_1 and L_2. DPOAE can be measured in the ear canal with a sensitive microphone.

In humans, the most pronounced DPOAEs are observed at the 3rd order intermodulation product frequency $f_{DP} = 2f_1 - f_2$. In clinical practice, DPOAEs are used as a diagnostic tool to evaluate the function of the cochlear amplifier (Davis, 1983), typically with fixed frequency ratio set to approx. $f_2/f_1 = 1.2$ to maximize response amplitude (Gaskill and Brown, 1990).

Several approaches have been made to establish an optimal standard paradigm for DPOAE measurements to assess the state of the so-called cochlear amplifier. These approaches can be described by the dimension of the parameter space (Mills, JASA 112, 2002).

The method most commonly used in clinical settings, known as a DP-Gram, measures DPOAE at a single combination of stimulus levels (often $L_2, L_1 = 55, 65dB$ SPL) for each frequency (Abdala, 2001), and thus represents a one-dimensional scan. The diagnostic information sought, i.e. the state of the cochlear amplifier, has a highly nonlinear and quite variable relation to the DPOAE amplitude (Gorga et al. 1996, Bhatt et al. 2023). Therefore, a normative range is defined within which the amplitudes should fall if the cochlear amplifier is functioning normally. This approach leads to a dichotomous diagnostic result, indicating whether or not the cochlear amplifier is healthy (Probst et al., 1991, Lonsbury-Martin and Martin, 2003 in Current opinion in otolaryngology head and neck surgery).

A more advanced approach, DPOAE input-output (I/O) functions, uses multiple level combinations where the stimulus-tone levels are linearly related (Kummer et al., 1998), and thus adds a second dimension. In this method, the DPOAE pressure responses are plotted as a function of the level of the second primary. DPOAE input-output (I/O) functions enhance diagnostic sensitivity for detecting cochlear-amplifier-related hearing loss (Gaskill and Brown, 1990; Stover, 1996, Gavin & Dhar, 2024, JARO). When extrapolated from semi-logarithmically scaled I/O functions, this approach provides

an almost linear relationship between DPOAE threshold and pure-tone hearing threshold (Boege & Janssen, 2002; Gorga et al., 2003). Importantly, this method allows the use of inclusion criteria that are independent of signal-to-noise ratio (SNR) thereby improving diagnostic yield and accuracy (Zelle et al. 2017).

Finally, DPOAE can be sampled at a range of independent level combinations creating a three-dimensional representation in the (L_2, L_1)-plane, thus adding a third dimension to the data recorded per given frequency f_2.

This approach, which we refer to as DPOAE level map (LM) was initially introduced by Whitehead (1995) and Kummer (2000). DPOAE LMs of limited density or extent can also be derived from investigations on DPOAE amplitude dependence on one stimulus level alone, e.g. [Brown & Gaskill, 1990, Neely 2005]. All mentioned reports used prescribed level combinations, which we refer to as static level maps (SLMs), to investigate DPOAE generation characteristics, primarily focusing on identifying group-optimal stimulus paths in the (L_2, L_1)-plane that lead to maximum DPOAE levels. Zelle et al., 2015 reported on DPOAE LMs based on pulsed DPOAE using the onset decomposition (OD) method that eliminates artefacts caused by the interference of the two competing source contributions: the nonlinear-distortion component and the coherent reflection component [Zelle, Thiericke 2015]. The OD method samples the rising onset of the DPOAE signal in the time domain before the low-latency reflection component begins to interfere. As a result, "smooth" DPOAE LMs with a clear maximum allow a more precise representation of the state of the cochlear amplifier and thus increase the diagnostic yield and accuracy (Zelle et al., 2015, Zelle et al., 2020).

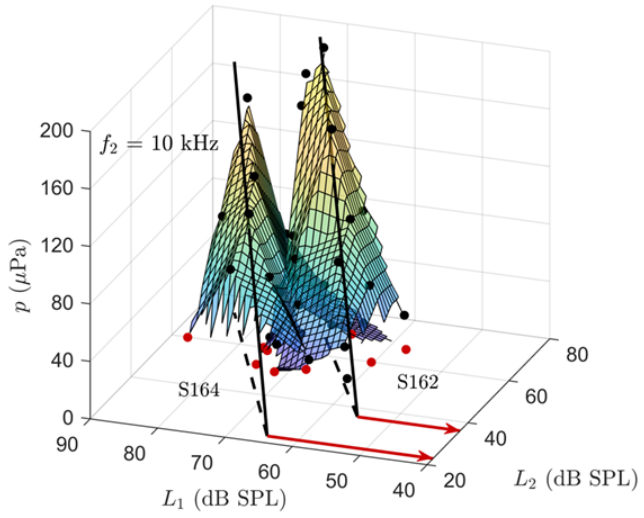

Fig. 1. Two DPOAE level maps measured in different normal-hearing subjects at $f_2 = 10kHz$. These DPOAE LMs demonstrate cases from the study of Bader et al., 2021, where a reasonable measurement of I/O functions (black, continuous lines) cannot be achieved with one common group-optimal stimulus path in the (L_2, L_1)-plane, lying somewhere between the individual optimal stimulus paths (dashed black lines). The black solid lines are referred to as ridges of the DPOAE LMs.

B. DPOAE level dependence

Experimental evidence from multiple studies (Cooper 1997, Whitehead 1995, Kummer 2000, Zelle 2015, Zelle2020) indicates that DPOAE LMs in mammalians, including humans, exhibit a common characteristic, particularly at low-to-moderate stimulus levels ($L_2 < 50dB$ SPL). This characteristic manifests as a distinct ridge (see Fig.2A) representing the maximum DPOAE amplitudes stimulated by the minimal stimulus pressure, i.e. at optimal combinations of L_1 and L_2. The ridge's projection onto the (L_2, L_1)-plane yields the level combinations that can be considered individually optimal for each ear (Zelle 2020).

The structure of DPOAE LMs can be roughly approximated by a 5-parameter model (ref patent Ernst & Zelle 2020). This model implies that the ridge is a line in a defined (L_2, L_1, p_{DP})-space with parabolic cross section when DPOAEs are scaled as level ($L_{DP} = 20log_{10}(p_{DP}/20\mu Pa)$, with p_{DP} being the sound pressure of the DPOAE). The line itself is described by four parameters: (a, b, s and $L_{2,EDPT}$), where s is a slope in $\mathbb{R}^3$-space, a the slope of the optimum path in the (L_2, L_1)-plane, b is its L_1-intercept, and $L_{2,EDPT}$ is the intercept of the ridge line with the (L_2, L_1)-plane (edpt: estimated distortion product threshold). The cross-section perpendicular to the ridge and the (L_2, L_1)-plane is provided by a 5th parameter c, which expands the line to a model surface with a parabolic law dependent on the level of the DPOAE, L_{DP} (Zelle et al. 2020).

In experimental practice, however, the ridge of a DPOAE LM is not always a straight line, the shape of the surface can deviate characteristically from the 5-parameter model, and the ridge's position may vary significantly between individuals. Ridge position and slope are affected by pathological but also non-pathological middle-ear transduction changes, such as minor static middle-ear pressure changes (janssen et al., 2005, JASA 117). Together with off-ridge points characterizing the general shape of the map, the estimated ridge representing the DPOAE I/O function may provide the clinically most important information about the DPOAE LM, as it not only allows the estimation of the hearing threshold but also represents compressive nonlinearity and allows predictions about the functional state of the cochlear amplifier independent of threshold (Abdala et al., 2021). It is, though, understood, that the regular shape of DPOAE LMs can be compromised by several factors, e.g. spontaneous otoacoustic emissions (SOAE), SNR, or time variance during measurement.

C. Aim of a new method to derive DPOAE level maps

Traditional methods, which rely on predefined, i.e. static level combinations, may fail to capture the ridge of each subject's DPOAE response, or lead to time-consuming collection of data without any or important information. In this article we introduce a method for adaptive DPOAE LM acquisition that is capable of autonomous exploration of a LM based on the existence of DPOAE responses and their amplitudes, and that can be tailored to different research or clinical needs.

Another aim is to assess all forms of LMs not limited to a priori assumptions about their shape as those inherent in the

5-parameter model presented in [Zelle 2020], specifically with regard to the derivation of a subject-specific optimal path that might not necessarily be linear in the (L_2, L_1)-plane. With respect to clinical needs, the adaptive scanning algorithms investigated here might serve in future to collect DPOAE data containing the complete three-dimensional information in a most time-efficient manner.

The LM approach requires the measurement of more DPOAE than a DPOAE I/O function. In turn, it offers two significant advantages: 1) Measuring a LM reveals the individually optimal path. Once known, a measurement of an I/O function along this path or its derivation from the DPOAE LM provides a more accurate representation of DPOAE growth properties compared to measurements of DPOAE I/O functions along a group-optimal path (s. Fig.1 and Zelle et al., 2020). Figure 1 shows an example of maximally separated DPOAE LMs from two normal-hearing subjects which would lead to misleading results when measured with DPOAE I/O functions along one group-optimal path. 2) Characteristic shifts of the DPOAE LM and accompanying reductions of the amplitudes of their ridge are known to be produced by conductive hearing loss, i.e. reductions of middle-ear transmission, and can therefore potentially be used for differential diagnostics of middle- and inner-ear impairments and lead to higher specificity for the diagnosis of the state of the cochlear amplifier (Janssen et al., 2005, Kummer, 2006, Turcanu, 2009, Steffen, 2017).

The here introduced adaptive measurement algorithm considerably optimizes the time required for data acquisition, making it a more efficient and reliable method for clinical diagnostics and research.

II. Methods

A. Measurement system and calibration

OAE measurements were conducted bilaterally using an ER-10C DPOAE probe system (Etymotic Research, Elk Grove Village, IL, USA), connected to a 16-bit analog output card and a 24-bit signal acquisition card (NI PCI 6733 and NI PCI 4472, National Instruments, Austin, TX, USA), all housed in a standard PC. The sampling rate was set to 102.4 kHz. Stimulus generation, data collection, and signal post-processing were carried out using a custom MATLAB toolbox ("DPAOE-Creator", version 24.2, MathWorks, Natick, MA, USA). The sound pressure of the ER-10C speakers was determined through in-ear SPL calibration, repeated every 600 seconds. Additional details about the calibration procedure can be found in (Zelle et al., 2015a).

B. DPOAE acquisition – Static level maps

SLMs are DPOAE LMs that are recorded using predefined (L_2, L_1)-stimulus level combinations. The aim is to capture the expected position of the DPOAE LM with an appropriate region around the ridge, based on the population mean parameters of the group optimum path for different frequencies. The stimulus level combinations for SLM were adapted from (Zelle 2020) and slightly modified especially at high stimulus levels. The resulting grid had lateral symmetry about the expected group-mean optimum path (L_2'-axis, cf. Fig.2B), fixed distances ($10dB$ along the L_2'-axis, and $6dB$ along the L_1'-axis). It comprises six cross sections of the expected level map with 3, 4, 5, 3, 3, 3 points per scan along the L1'-axis (see Fig.5, red pattern). The position of the grid is defined by $(L_{2,MIN}, L_{1,MIN})$, s. Fig.5, for values, s. Sec. V, Table 1), which were based on the experience from previous experiments (Bader et al., 2021) to optimize data yield in normal-hearing subjects.

C. DPOAE acquisition – Adaptive level maps

Adaptive LMs (ALMs) are defined as DPOAE LMs that are procedurally generated to increase the efficiency of DPOAE acquisition. After measuring a prescribed starting point, the algorithm selects the next stimulus level combinations based on the configuration of assessed data and their relation to an expected LM shape. This is accomplished by comparison of accepted DPOAE, i.e. those with $SNR \geq 10dB$, with the 5-parameter model defining the a priori expectance of a LM shape.

An initial level combination (i.e. p_1^1 on Fig.2B) is chosen in a frequency-dependent manner with$L_{2,START} = 55dB$ for $f_2 < 4kHz$, 60 dB for $f_2 < 8kHz$, and $65dB$ for larger f_2, while L_1 is chosen to lie $6dB$ below the group-optimal level according to Zelle et al., 2020 (see Table I, Sec. V I). In principle, all adaptive methods described in the following can be utilized stand-alone or in conjunction, depending on the particular clinical or research task. We subdivide the adaptive methods into two groups.

The first group of ALM acquisition methods relies on the expected shape of a DPOAE level map, i.e., it uses a priori knowledge as discussed in Section I.C, and shown in Fig.2A. Two methods belong to the a priori group: the so-called ridge estimator and ridge follower. To simplify the description of the ALM methods, we refer to a (L_2', L_1')-plane which is rotated such that the projection of the ridge onto the (L_2, L_1)-plane aligns with the L_2' axis (s. Fig.2B). The angle of the rotation corresponds to the group mean parameter a of the 5-parameter model (s. Sec. I.B, and Zelle 2020).

The ridge estimator (ref to patent) is utilized to verify the presence of the presumed DPOAE LM and to roughly estimate model surface properties. The algorithm is comprised of three steps – two ridge scans and one intermediate point (see Fig. 1A for ridge and Fig.2B for illustration of the ridge estimator algorithm):

1: An initial ridge scan p_k^1 samples the presumed ridge along L_1' starting from an initial level combination p_1^1 and aims to detect its maximum to prove the existence of a ridge. Every single ridge scan might take up to k DPOAE amplitudes or points (here: $k = 4$), limited by a predefined region of interest (ROI). The ROI might be tailored to specific tasks, but typically will contain an upper limit for L_2 and L_1 to avoid acoustic overstimulation and/or technical distortions (here: $95dB$ SPL). Sampling during a ridge scan has two modes: 1) if there are no accepted DPOAE amplitudes or points, the L_1' increment is set to $10dB$, 2) if the acquired DPOAE adhere to the predefined

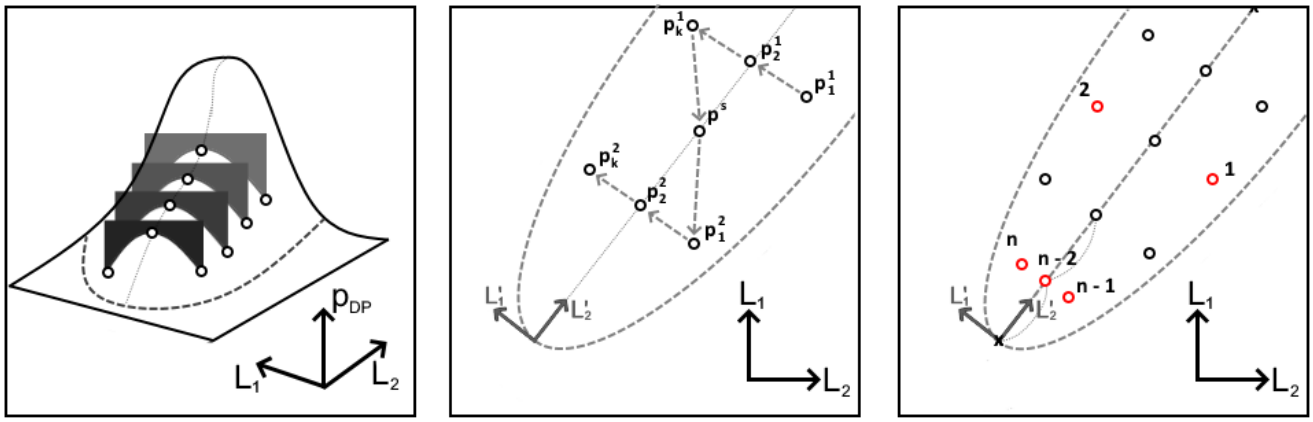

Fig. 2. Model-based algorithms to identify the ridge of DPOAE LMs: A: Model surface of an ideal DPOAE LM, described via perpendicular scans, illustrating the expected structure of a typical DPOAE LM. B: Ridge estimator method. To minimize the number of points per measurement, this method employs two ridge scans ($\boldsymbol{p_i^1}$ and $\boldsymbol{p_i^2}$) and one intermediate point $\boldsymbol{p^s}$. Ideally, it samples seven points to estimate all major characteristics of the DPOAE LM. C: Ridge follower method. This method strongly relies on the estimated DPOAE LM surface and is used to enhance the resolution of points along the ridge. It requires a minimum of three points per scan (the ridge point and one point on either side) and provides a prescribed overall amount of scans perpendicular to the ridge.

acceptance criteria (based on SNR, s. Sec. II.D), the L_1' increment is set to $6dB$. If the detected DPOAE amplitude p_{DP} decreases after two successful measurements, the L_1' increment is switched to be negative. Once three DPOAE have been accepted, the maximum is determined by solving a quadratic equation to their levels. If four attempts fail to determine a ridge, an additional scan is deployed on half distance between the existing scan and upper ROI boundaries.

2: Once a maximum within a ridge scan is detected, an intermediate point p^s is sampled to estimate individually the slope of the ridge. This point is positioned based on the assumed frequency dependence of the slope s of the group mean optimal path, a (Zelle 2020, their Table I) and on the typical background noise levels – such that it is expected to fall on half distance between the first scan and the location where the prescribed minimum SNR for an accepted DPOAE would be obtained. In this study, SNR_{MIN} was set to $10dB$.

3: After the slope of the DPOAE LM ridge is individually computed, a starting point for the 2nd low-level scan perpendicular to the ridge is set at a L_2' where a $SNR = SNR_{MIN} + 12dB$ is expected. This value was chosen empirically as a compromise between the goals to obtain valid DPOAEs at low stimulus-levels and to avoid measuring neighbouring off-ridge points without achieving the required SNR. After measuring an initial point, the second scan p_k^2 is performed in the same manner as p_k^1 (see step 1).

The second acquisition method of the *a priori* group is the ”ridge follower”. This method involves two recurrent steps (see Fig.2C) aimed at enhancing the resolution of the DPOAE data along the ridge:

1: For any existing singular point on the ridge (e.g., p^s in Fig.2B), two satellite points are assigned on either side of the ridge. There can also exist other incomplete scans because the presumed ridge which is calculated by the 5-parameter model, may have shifted during the procedure. Therefore, after recalculation of the model, no point within a scan is situated within $\pm 1dB$ of the calculated ridge, a new ridge point is measured. This choice was done in order to ensure that a growth function along a linear path can be constructed without interpolation.

2: If no singular points are left, a new point (s. Fig.2C: n–2) is positioned on the ridge. The longest empty interval, either between the ROI boundaries and the nearest point or between existing points along the ridge, is identified, and the new point is placed by bisecting the interval.

A second group of ”data-based” acquisition methods was implemented, relying solely on the already existing points based on Delaunay triangulation (Lee, D.T., Schachter, B.J., 1980) referred to as”polygonal search method” (PSM). The PSM and terms used in the following are borrowed from graph theory. It comprises two cases – the general and the expansive case.

In the general case of the PSM (see Fig.3A), any existing points with all kind of DPOAE amplitudes within the boundaries of the ROI are considered. The data-based algorithm consists of the following steps:

1: All points which have already been measured (continuous-line circles in Fig.3A, $p_{1\ldots3}$), are processed with a Delaunay triangulation function (matlab function *delaunayTriangulation(P)*) that generates triangle polygons, based on those and defined via vertices coordinates list and triangular face connectivity list (Lee, D.T., Schachter, B.J., 1980; see their Appendix B).

2: To construct polygons adjacent to boundaries of the ROI, the vertices of the alpha shape of all acquired points, i.e. the circumference of the set of triangles, are connected to the boundaries of the ROI according to the minimum-distance principle (vertical and horizontal lines in Fig.3A). To prevent edge clustering, the (L_2, L_1)-plane is divided

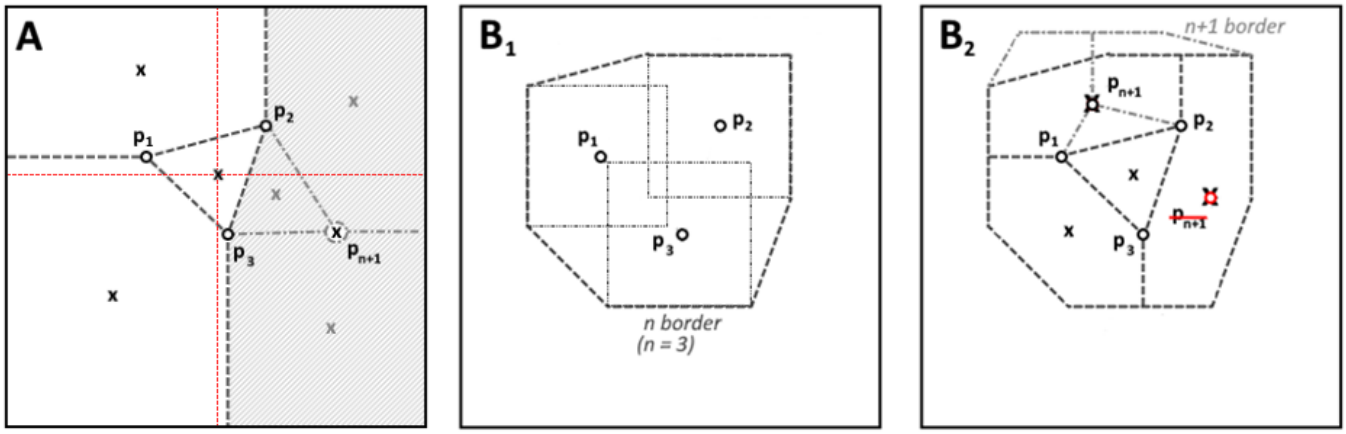

Fig. 3. Data-based algorithm to identify DPOAE LM without a priori assumptions on its shape. A situation may arise where certain points have been measured, but the model surface cannot be accessed. In such cases, an algorithm is used that systematically searches for data points in the $(\boldsymbol{L_2}, \boldsymbol{L_1})$ level depending on the SNR. A: The general case of the Polygonal Search Method (PSM) splits the ROI into smaller polygons and takes the centre of mass ($\boldsymbol{p_{n+1}}$, marked as cross) of the biggest polygon (gray hatched area) to be measured next. B: An expansion case of PSM is a stricter version of general case, which bases its prediction only on "accepted" points. It generates the boundary (n border), by using square regions of vicinity around "accepted" points. C: Inside the boundary, the general case of the PSM (A) is applied to find the next point to be measured.

into four sections by two orthogonal lines (see red dashed lines in Fig.3A) intersecting at the centre of mass of the alpha shape. Points can only be connected to a boundary located in the same section.

3: Once all connections between the points and the boundaries are established, the updated connectivity list contains all non-overlapping polygons within the ROI. The largest polygon (see gray polygon in Fig.3A) is selected and its centre of mass is chosen as the next measurement point.

If PSM is applied without prior data, the subdivision of the (L_2, L_1)-plane (step 2) begins in a pre-described initial point and creates four different polygons. Following this step, the method continues with the aforementioned steps.

In the expansion case of the PSM, only points with accepted DPOAE amplitudes are taken into account and the ROI is re-defined based on those points in every step. For each accepted point, neighbouring points defining a group are identified by their distances with $\delta L_2 \leq 10dB$, $\delta L_1 \leq 15dB$. Around these points, a square-shaped region of pre-defined size is built (here: $20 \times 20dB$), and their common circumference is yielding a polygon, which describes the new ROI (s. Fig.3B, dashed line). Following these rules, more than one ROI can appear. The final step is to employ the general case for all groups simultaneously, meaning that the largest polygon identified in any group generates the next point (s. Fig.3C). The expansion case has the advantage to constrain the ROI to an area where the probability might be deemed high to lead to accepted DPOAE.

D. Study design and subjects

The pilot study, validating the adaptive algorithm for DPOAE LM acquisition, included three normal-hearing subjects (age: 27, 31 and 37 years old). All three subjects were classified as normal-hearing as all pure-tone thresholds were better than 20 dB hearing level (dB HL) for frequencies between 1 and 8 kHz.

DPOAE LMs were recorded bilaterally at 14 frequencies ranging from 1 to 14 kHz ($f_2 = 1, 1.5, 2, 3, 4, 5, 6, 8, 9, 10, 11, 12, 13, 14kHz$), yielding 84 independent data sets. The stimulus and recording sequence are based on a time-interlaced multi-frequency acquisition technique (Zelle, 2014). 21 level combinations per frequency were chosen, each of which averaged over 44 ensembles comprising four blocks with appropriate phase shifts to apply the PTPV technique. Within a block of length of 0.18 seconds, 7 frequencies are presented in a time-interlaced manner; the whole measurement including intermittent calibrations took approximately 25 minutes. For each measured DPOAE amplitude, we performed sorted averaging, estimated the noise floor and, if SNR exceeds 10 dB, the corresponding point was considered accepted. The noise floor was estimated as the root-mean-square of the difference between two subsets of the underlying segments from the DPOAE recording in a 50-ms time interval centred on the DPOAE response. The subsets were created by averaging two sets of interlaced PTPV ensembles, each of which contained four consecutive segments with suitable phase variations to cancel the stimulus pulses.

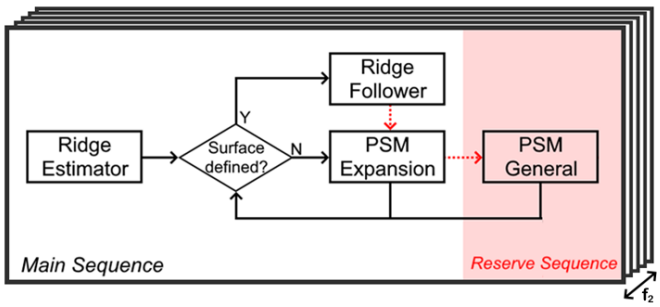

Fig. 4. Adaptive acquisition workflow: Black arrows – regular sequence, red arrows – exception sequence (if measurement at prescribed point is not possible for any reason).

The sequence of measurements used in this study is depicted in Fig.4. After assessment of pure-tone thresholds using a Békésy tracking method (for details: Bader et al., 2021) , DPOAE are acquired with ALM followed by SLM in a subsequent visit after 1-2 months. During ALM acquisition (see Section II.C), the sequence of *a priori* and *data-based* acquisition methods is followed independently for each frequency stimulated within a block. The sequence is organized so, that after completion of the ridge estimator, the model is fitted to all previously assessed DPOAE amplitudes after each measurement. The 5-parameter model is accepted if the following criteria are met: $r^2 > 0.8, \sigma \leq 10$, where r is the correlation coefficient between DPOAE amplitudes and the 5-parameter model fitted to them, and σ is standard error of the model parameter $L_{2,EDPT}$ (Zelle et al., 2020; see Section I B). If these criteria are satisfied, the ridge follower algorithm complements the level map, if not, the PSM expansion method is initiated.

The study was approved by the Ethics Committee of the University of Tübingen and was conducted in accordance with the Declaration of Helsinki for human experiments.

E. Post-processing and analysis

1) Connectivity-based analysis: To compare and analyse SLM and ALM without relying on the surface shape produced by the DPOAE, we use quantities that are present in each measurement: number of all acquired points (N_{all}), number of points with accepted DPOAE amplitudes (N_{acc}), and the area of the alpha shape (S) of N_{acc} (s. Fig.5). Additionally, for post-processing here we restrict the connectivity list such, that it does not have triangles with edges larger than 18 dB, to minimize the influence from extrapolation artefacts, which might take place in next subsection.

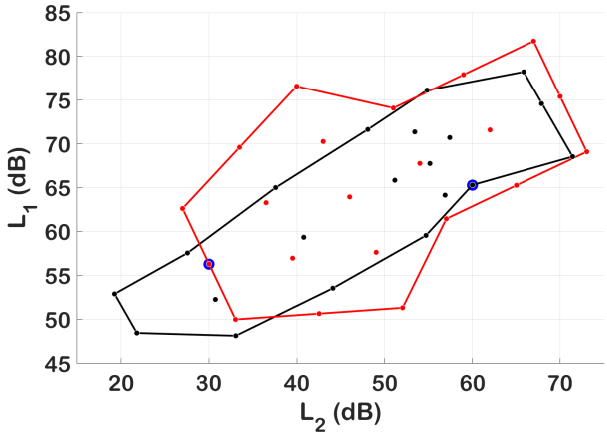

Fig. 5. Accepted points and their correspondent alpha shapes: adaptive (black) and static (red) level maps. Initial points for both approaches are highlighted with blue circles. An ideal scenario where all points meet the acceptance criteria, and the level maps do not clip to the ROI boundaries.

Time efficiency of an LM measurement is defined here as the ratio of accepted points to all acquired points (N_{acc}/N_{all}). The second metric is used to assess a "goodness" of coverage. Together with S, the areal density of the points with accepted DPOAE amplitudes ($\rho = N_{acc}/S$) creates a (ρ, S)-space, where the main underlying assumption is, that there exists an ideal LM with ideal values, i.e. (ρ_{max}, S_{max}), where ρ_{max}, S_{max} are the maximum values of these variables across all LMs (here 6 ears x 14 frequencies x 2 methods). In this context, any reduction in Nacc leads to a value below one. Similarly, any dispersion over a larger area S in the (L_2, L_1)-plane leads to a value below one. The latter criterion $\rho < 1$ is here taken as an indicator of loss of information.

2) Comparison of obtained maps: First, the accepted points, acquired with SLM and ALM, are interpolated using biharmonic splines (X. Deng, Z. Tang, 2011). For ridge identification, the measured LM is transformed into a gradient field. A simplified version of the Dijkstra algorithm (Dijkstra, E.W., 1959) is used to trace the path with the least inclination from the peak towards lower values. The customized algorithm includes the following simplifications: it operates on a predefined mesh graph, only allows movement towards lower or equal L_2 values from the initial point, has an open end instead of searching for a distant endpoint, and considers only neighbouring nodes of the mesh. To reduce oscillations and enhance stability, additional weighting is applied to the gradient field based on two rules: 1) nodes with L_2 lower than initial point (close-range interaction bias $= 0.995$) and 2) nodes, which are closer to the line connecting the initial point to the closest local minimum on gradient field, have their weight additionally modified (long-range interaction bias $= 0.9$).

To compare LM shapes obtained via different methods, we need a common measure that incorporates all the evaluated data.

This is achieved by applying a joint polynomial fit to the ridges obtained by the SLM and the ALM method. Each ridge is fitted to its own polynomial with k characteristic low-order terms and iterative $n-k$ shared higher-order components. The order of the polynomial is incremented by 1 and is limited by $k = 1$, $n_{max} = 15$.

$$\begin{cases} p_n x_\alpha^n & + p_{n-1} x_\alpha^{n-1} + \cdots + p_{k+1} x_\alpha^{k+1} \\ & + \alpha_k x_\alpha^k + \alpha_{k-1} x_\alpha^{k-1} + \cdots + \alpha_0 x_\alpha^0 - y_\alpha = 0 \\ p_n x_\beta^n & + p_{n-1} x_\beta^{n-1} + \cdots + p_{k+1} x_\beta^{k+1} \\ & + \beta_k x_\beta^k + \beta_{k-1} x_\beta^{k-1} + \cdots + \beta_0 x_\beta^0 - y_\beta = 0 \\ & \vdots \end{cases} \quad (1)$$

The k-fold cross-validation is used to prevent overfitting, where amount of folds is selected dynamically based on size of data (with minimum four and maximum ten folds). When one of the lines is considered to be overfitted, then previous state is taken as a result.

A common ridge is then determined by fitting the remaining free components using the previously identified higher-order terms. The final step is to calculate the distances of points to the joint fit of the ridges of SLM and ALM methods (see Fig.6).

III. Results

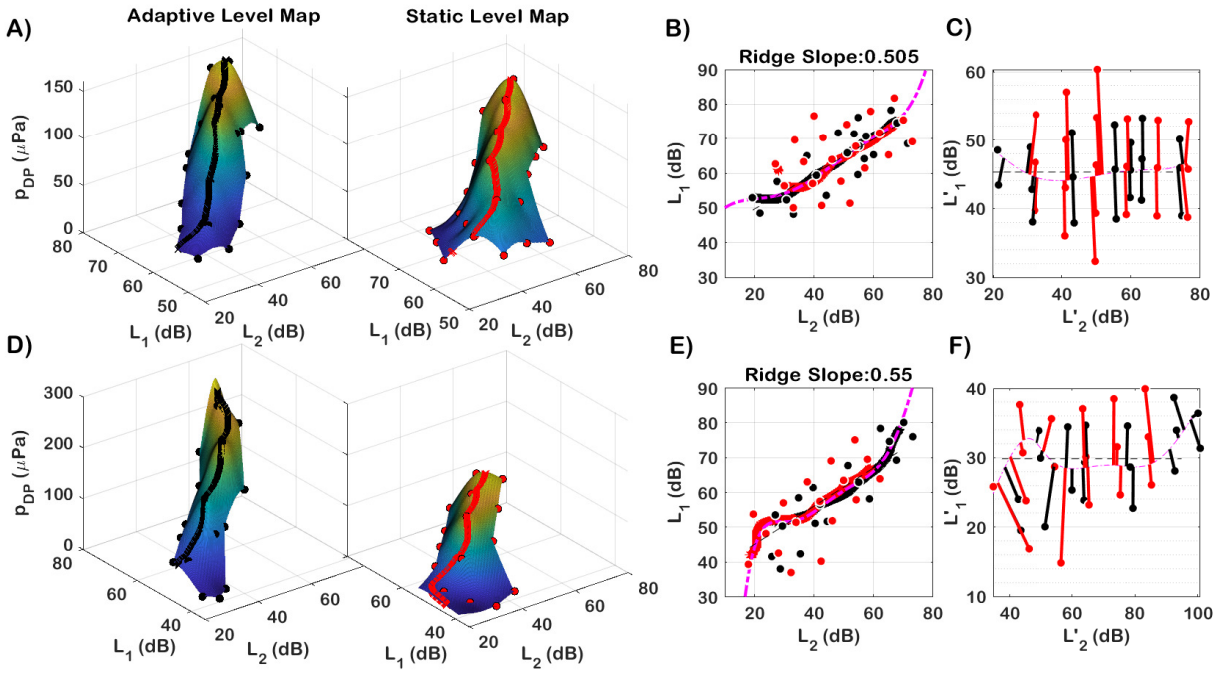

Fig. 6. Comprison of feature identification with SLM and ALM method. A, D: A level map interpolated with biharmonic splines and its ridge, estimated using the "ridge searcher" method. B, E: Estimated ridges from the LMs in A, D and a general ridge derived through iterative polynomial fitting of these two ridges. C, F: Distances between the general ridge and measured points for both maps. A–C: represent a nearly ideal case (S345, 4 kHz), where the data are centered to the sampling grid for both methods, whereas D–F show a more typical result of LM acquisition, where the sampled area differs more clearly between both methods. (S345, 2 kHz).
Black color – ALM, Red color – SLM.

A. Qualitative features of the interpolation and ridge comparison method

Fig.6A-C and Fig.6D-F show two examples of LMs pairs obtained with the adaptive (black curve) and the static (red curve) method. The upper example (Fig.6A) illustrates an acquisition of a nearly ideal level map. For both, the ALM and the SLM, all measured points met the SNR criterion (only points, passing the SNR criterion, are connected by the mesh illustrating the surface in (Fig.6B)). The interpolation method used introduces rippling along the ridge, which putatively does not reflect the true shape of the level map, and should be considered as an artefact resulting from the spline interpolation method. The black and the red line designate the result of the ridge search algorithm (see Section II.E). In the upper example (Fig.6A–C), the ridge lines cut almost always through the central points of the sampling grid for both methods, whereas for the bottom example, this is the casse only for the ALM method. Nonetheless, the ridges are almost identical where the data overlap.

An example where SLM and ALM methods have led to slightly different area coverage is shown in Fig.6D. Fig.6B and E show the projection of the identified ridges and the stimulus level pairs of accepted points onto the (L_2, L_1)-plane. In the upper example, the ridges of both, ALM and SLM, align closely and correspond to almost straight lines. However, in Fig.6E, the area covered by the SLM method is shifted toward lower L_2 values, especially at high levels. Nonetheless, the ridges identified by both methods are very close to each other in the area where both methods contribute. The projection of both ridge identifications onto the (L_2, L_1)-plane shows that the ALM technique succeeds in capturing the ridge on its center line of the sampling grid in both examples.

B. Acceptance rate and time efficiency

Fig.7A shows the acceptance rate (Nacc/Nall), representing the portion of points that passed the $10dB$ SNR criterion, across all six ears, dependent on frequency. In general, ALM measurements resulted in a greater number of accepted points at most frequencies, the exceptions being 3, 12, and 13 kHz. Fig.7B shows the histogram of the acceptance rate within a single LM across all frequencies and all ears. ALM show in 36% of all LMs an acceptance rate of ≥ 0.95, i.e. 20 out of 21 or all points which have been tested passed the SNR criterion, while the correspondent figure for SLM was only 10%. The median of the acceptance rate was 0.62 and 0.78 for SLM and ALM indicating that ALM is more effective in setting stimulus levels to achieve DPOAE signals with SNR $\geq 10dB$ compared to SLM.

Overall, we obtained 1020 accepted DPOAE amplitudes with SLMs and 1258 accepted DPOAE amplitudes with ALMs, indicating a 23% increase in quantitative output.

C. Coverage of DPOAE LMs

To compare the relative performance of both methods, we performed a joint analysis of the area, defined by the alpha shape corresponding to the accepted points, and their (L_2, L_1)-density (see Section II.E). Both values (ρ, S) are min-max

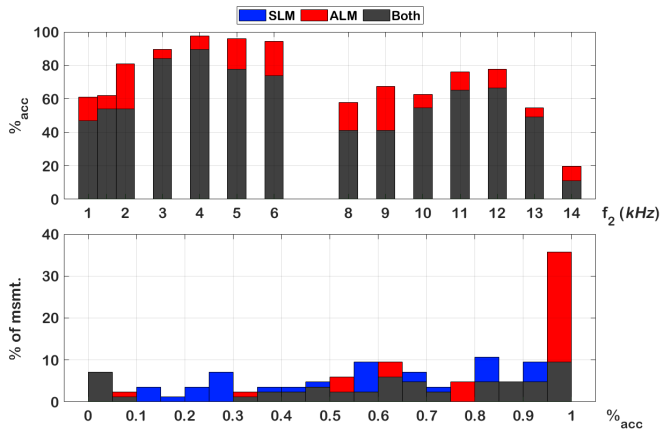

Fig. 7. A) Share of accepted points over frequencies for all ears. B) Distribution of percentage of accepted points per single LM measurement for all frequencies and ears. Black color shows the method with the smaller or equal share. The ALM method contributes more accepted DPOAE determinations at all frequencies (panel A), and it succeeds in 36% of the cases to provide 95–100% valid DPOAE, i.e. in theses cases at least 20/21 DPOAE measurements within a given LM were reaching the SNR criterion, as compared to only 10% for the SLM method.

normalized in linear space and converted to log space (see Eq.2):

$$log(\rho) = log(\frac{\rho - \rho_{min}}{\rho_{max} - \rho_{min}}); log(S) = log(\frac{S - S_{min}}{S_{max} - S_{min}}), \quad (2)$$

where the minimum and maximum values are determined separately for each LM. Thus, in linear space, ρ and S cannot attain values of > 1, or equivalently their logarithm cannot become > 0. Therefore, a deviation of any of either parameters towards "$-\infty$" designates a loss of information.

Fig.8 shows a bivariate histogram of area and density for the obtained LMs, with the left panel representing ALM, and the right panel representing SLM. The majority of measurements (clustered with brightest square as a centre) acquired with the ALM method is shifted closer towards $(0, 0)$, compared to those obtained by the SLM method. This shift suggests that ALMs prioritizes point density over area coverage, resulting in an improved resolution of the LMs close to the ridge.

Fig.9 shows the cumulative distribution of the distance of the (L1, L2)-coordinates of accepted points from the ridge. For ALM, 74% of the accepted points lie within $6dB$ from the ridge, compared to only 54% for SLM. Moreover, in the static methods, more than 20% of points are over $8dB$ away from the ridge. Taking a typical level map cross section given by $L_{DP} = -0.12\delta L_1^2$ (Eq. 4 and Tbl. I in Zelle, 2020), $8dB$ off ridge suggests already a relative loss in SNR of $7.7dB$, compared to only $4.3dB$ for $6dB$ distance.

Fig.10 shows the performance of the four adaptive acquisition methods in the implementation used here, given as statistics of the ratio of accepted points collected by a single method to all accepted points within a given LM. For the both lower frequency ranges, judged by the median, more than 80% of the accepted points were successfully acquired by the a priori methods (ridge estimator and ridge follower), whereas the adaptive acquisition workflow (Fig.4) only seldom needed to invoke the data-based algorithms. On the contrary, for the high-frequency range, as judged by the median, only 36% of the accepted points were contributed by the a priori methods, whereas the data-based methods gained importance and contributed 19%.

IV. Discussion

This study pursued two major goals: First, design and evaluate an adaptive level-map acquisition method that is able sample the LM where DPOAE with acceptable SNR can be obtained. The second goal was to develop and investigate a method for characterization and comparison of LMs obtained by different methods without limiting the comparison to a priori assumptions on their shape such as the 5-parameter model.

A. Method advantages and drawbacks

In most or probably all medical imaging techniques, the acquisition of the data, even when not measured simultaneously in a single capture, is not designed to depend on the data themselves. At best, the region of interest is planned in advance to meet the needs of an individual patient. For DPOAE-acquisition, a simultaneous acquistion is largely not realizable because of the nonlinear interactions inside the cochlea, and, for a single parameter set (frequencies, levels, etc.), the necessary recording time can already take 1 minute depending on the DPOAE's level, thus rendering acquisition of 3D information extremely time consuming.

Therefore, the ALM method presented here are designed to extract only the features deemed relevant from the resulting LM while avoiding as much as possible to measure at stimulus levels where sufficient SNR cannot be reached within the prescribed time. To address this, we employed a two-stage search sequence, consisting of pattern recognition (a priori) and exploratory (data-based) methods. The a priori methods have proven to work well at all frequencies, but especially at frequencies at and below 8 kHz where they contributed more than 80% of the DPOAE with acceptable SNR.

Here, the exploratory methods have been used in the case that the a priori methods failed to identify a LM of the expected structure (as judged by the 5-parameter model). The concept of the exploratory methods might be seen analogous to the one shown in Fig.2A-B of Chiang, J. Y, 1997, where the sampling grid of a pattern recognition task first covers the entire image and then becomes finer in areas to capture the relevant features more accurately. While theirs and our methods differ in their implementation and execution, they share a common structure and topology, as both methods use a simplified beta skeleton of the data, which is a subset of the Delaunay triangulation that can be reconstructed into a polygonal surface (Eppstein, 1998). This dynamic approach allowed us to obtain useful data in the case that the a priori methods did fail where they could have been successful (this appeared in x cases), or a number of valid DPOAE that could be used for diagnosis even though they do not allow a valid model fit.

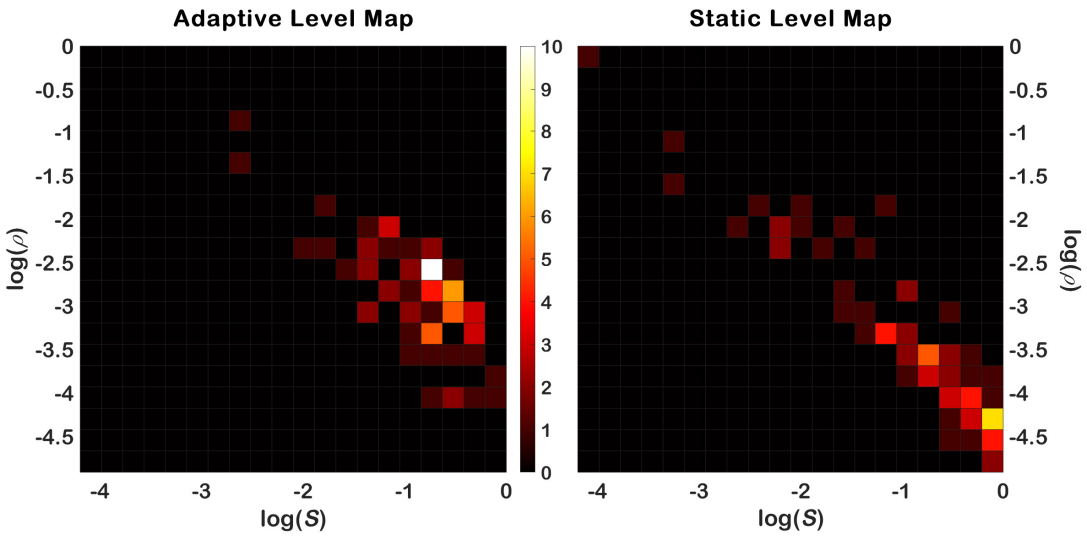

Fig. 8. Bivariate histogram of level map areas and their corresponding point density. This histogram is representing the qualitative aspect of LM properties which were encountered oin this study. There is an assumed ideal LM with largest area and density, which is located in $(\mathbf{0}, \mathbf{0})$, but cannot be obtained with the given amount of N_{all}. The colour scheme ranges from black through red to white. Higher colour intensity designates higher amount of counts.

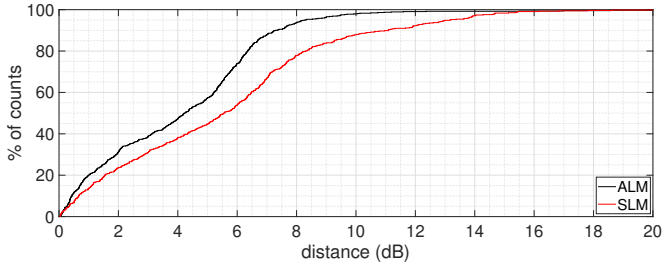

Fig. 9. Empirical cumulative distribution function of the distances between the estimated ridge and measured points for all LMs where both, ALM and SLM, passed the acceptance criteria for identifying a ridge (each ridge length must be more than $\mathbf{12}dB$ and both - ALM and SLM ridges - must exist)

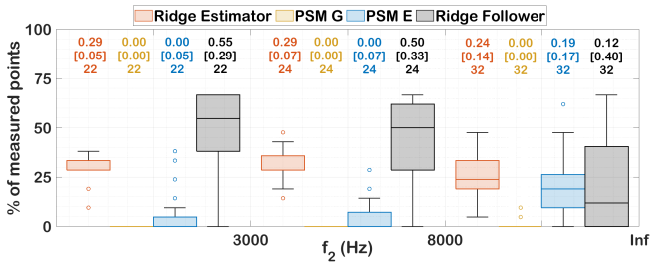

Fig. 10. Median, interquartile ranges, and range of the share of accepted DPOAE within a level map which was obtained by the four adaptive acquisition methods, grouped into three frequency ranges. Numbers above the box-whisker plots are: Median, interquartile range, and amount of datasets containing at least 6 accepted DPOAE, which were 78 out of 84 possible datasets.

B. Time concern

It might be instructive to consider two cases, a typical clinical and a typical research application. In a routine clinical application, more than some 7 to 9 points per level map will probably be undesirable, because with a typical amount of 6–8 test frequencies, extrapolation of the figures given in Sec. II.D would lead to a measurement time of 3min35' to 6min8' in the current implementation. According to our estimation, by further optimization of the implementation, i.e. reducing measurement time where in the current implementation excessively high SNR are obtained, the measurement time could be reduced to below 4 min, what would be clinically practicable. The added use of the technique would then be: 1) Avoiding incorrect DPOAE growth properties due to applying individually wrong level combinations, 2) Obtaining an additional independent parameter, i.e. the relative position of the LM's ridge along the L_1'-coordinate, which is a marker for conductive hearing loss.

If we consider a basic research aim as, for instance, the characterization of individual LMs dependent on the frequency ratio f_2/f_1, one easily ends up with substantial measurements times: for instance, if one sets out for testing 5 different frequency ratios at 7 frequencies, and reduces the number of points per LM to 12, we find approximately 35' overall measurement time (calculated from the overall measurement time of 25' and the number of points per LM and frequencies used in this study, s. Sec. II D. The estimate depends on the mean frequency because of the pulse length definition.). This is a considerable measurement time which easily grows to more than an hour with more demanding requirements on sampling density of the different dimensions of interest, and at such high measurement times, the 12% gain in accepted DPOAE compared to SLM is highly useful (s. Sec. III B).

C. LM post-processing and analysis

To analyse LMs of different origins, we devised a toolset that largely avoids a priori assumptions, the only exception being a weak a priori assumption about its direction (Sec. II E), in the sense that the algorithm for the identification of the vector of least gradient, i.e. the ridge, preferes the direction

toward low L_2. The method generally worked stable and was able to identify all ridges where the 5-parameter model also achieved an acceptable fit . The metrics for evaluation of SLM and ALM method performance, that is, number of accepted DPOAE, coverage, and resolution of the optimum path, all show that the ALM technique worked well and superior to the SLM method. Of course, some of these metrics, especially what we call here the resolution of the optimum path, include partially sort of a self-fulfilling prophecy. By taking 6 dB as sampling step along the L_1' direction, the points gathered, if successfully, will be closer to the ridge compared to the SLM where the grid raster converted to an L_1'-value was 8 dB . On the other hand, the SLM has to make a compromise: If the grid raster becomes too fine, the number of LMs where the ridge cannot be identified due to its interindividual variation in position relative to the L_1'-axis, will rise, or, otherwise, a fourth and fifth line of samples has to be recorded along the complete range of L2-values. In this respect, the SLM method was already well optimized, having 4 and 5 samples orthogonal to the ridge at two low-to-moderate L2 stimulus levels, in order to reduce the probability of recording valid data without being able to fit the 5-parameter model to it.

With any reasonable amount of level combinations to be recorded, one has to make a compromise with regard to the resolution along and orthogonally to the ridge. Here, by our desgin of the ALM method, we chose basically an optimal grid of 3x7 points to characterise the ridge, if the a priori methods would be successful, which often was the case. The representation of the algorithm in the (ρ, S)-space is a suitable method to visualize the quality of any such method, because the compromise between two conflicting goals, a high point density and a high covered area is determined in 2D space. Especially here, the ALM method shows that a clearly better compromise has been achieved, and that much more of the LM acquisitions are positioned in higher proximity to the unachievable goal, i.e., reaching maximum density and high coverage at the same time.

V. Conclusion (SKETCH) (WORDS LIMIT = 300)

Here, we have introduced an adaptive method to acquire DPOAE LMs. DPOAE LMs are of clinical interest, because I/O functions derived from LMs are basically not affected by the choice of a group-optimal stimulus level path, and because conductive (i.e., middle-ear) loss might potentially be detectable, enabling a differential diagnosis that distinguishes it from inner-ear loss (Janssen, 2005, Marcrum, 2017, EarHear 38). On the other hand, LMs are important from a basic-research perspective for a more complete characterization of the distortion generation process. The comparison of these to the output of models of cochlear mechanics then can serve to evaluate and improve such models. The ALM technique has produced maps which are qualitatively equivalent to SLMs within the region of overlap, as judged by the identified ridges as well as by the rms-pressure difference between these maps within the overlap region. Simultaneously, the ALM data yield is considerably higher, in our study with normal-hearing subjects by x%... possibly: ...and has led to y% more DPOAE with acceptable SNR in case where the lowest stimulus level with acc. DPOAE was ¿=40 dB SPL. **(?)** Ultimately, the bivariate histogram of area and density has shown that the ALM makes a clearly better compromise between the both concurring goals, and that the compromise achieved is situated closer to the unachievable goal, i.e., reaching maximum density and high coverage at the same time.

VI. Template

A. Equations

Use one space after periods and colons. Hyphenate complex modifiers: “zero-field-cooled magnetization.” Avoid dangling participles, such as, “Using (3), the potential was calculated.” [It is not clear who or what used (3).] Write instead, “The potential was calculated by using (3),” or “Using (3), we calculated the potential.”

Use a zero before decimal points: “0.25,” not “.25.” Use “cm^3,” not “cc.” Indicate sample dimensions as “0.1 cm $\times$ 0.2 cm,” not “0.1 $\times$ 0.2 cm^2.” The abbreviation for “seconds” is “s,” not “sec.” Use “$\mathrm{Wb/m}^2$” or “webers per square meter,” not “webers/m^2.” When expressing a range of values, write “7 to 9” or “7–9,” not “7∼9.”

A parenthetical statement at the end of a sentence is punctuated outside of the closing parenthesis (like this). (A parenthetical sentence is punctuated within the parentheses.) In American English, periods and commas are within quotation marks, like “this period.” Other punctuation is “outside”! Avoid contractions; for example, write “do not” instead of “don’t.” The serial comma is preferred: “A, B, and C” instead of “A, B and C.”

If you wish, you may write in the first person singular or plural and use the active voice (“I observed that . . .” or “We observed that . . .” instead of “It was observed that . . .”). Remember to check spelling. If your native language is not English, please get a native English-speaking colleague to carefully proofread your paper.

Try not to use too many typefaces in the same article. You’re writing scholarly papers, not ransom notes. Also please remember that MathJax can’t handle really weird typefaces.

Number equations consecutively with equation numbers in parentheses flush with the right margin, as in (3). To make your equations more compact, you may use the solidus (/), the exp function, or appropriate exponents. Use parentheses to avoid ambiguities in denominators. Punctuate equations when they are part of a sentence, as in

$$E = mc^2. \tag{3}$$

Be sure that the symbols in your equation have been defined before the equation appears or immediately following. Italicize symbols (T might refer to temperature, but T is the unit tesla). Refer to “(3),” not “Eq. (3)” or “equation (3),” except at the beginning of a sentence: “Equation (3) is . . . .”

B. LaTeX-Specific Advice

Please use “soft” (e.g., `\eqref{Eq}`) cross references instead of “hard” references (e.g., `(1)`). That will make it

possible to combine sections, add equations, or change the order of figures or citations without having to go through the file line by line.

Please don't use the `{eqnarray}` equation environment. Use `{align}` or `{IEEEeqnarray}` instead. The `{eqnarray}` environment leaves unsightly spaces around relation symbols.

Please note that the `{subequations}` environment in LaTeX will increment the main equation counter even when there are no equation numbers displayed. If you forget that, you might write an article in which the equation numbers skip from (17) to (20), causing the copy editors to wonder if you've discovered a new method of counting.

BibTeX does not work by magic. It doesn't get the bibliographic data from thin air but from .bib files. If you use BibTeX to produce a bibliography you must send the .bib files.

LaTeX can't read your mind. If you assign the same label to a subsubsection and a table, you might find that Table I has been cross referenced as Table IV-B3.

LaTeX does not have precognitive abilities. If you put a `\label` command before the command that updates the counter it's supposed to be using, the label will pick up the last counter to be cross referenced instead. In particular, a `\label` command should not go before the caption of a figure or a table.

Do not use `\nonumber` inside the `{array}` environment. It will not stop equation numbers inside `{array}` (there won't be any anyway) and it might stop a wanted equation number in the surrounding equation.

If you are submitting your paper to a colorized journal, you can use the following two lines at the start of the article to ensure its appearance resembles the final copy:

```
\documentclass[journal,twoside,web]{ieeecolor}
\usepackage{Journal_Name}
```

The SI unit for magnetic field strength H is A/m. However, if you wish to use units of T, either refer to magnetic flux density B or magnetic field strength symbolized as $\mu_0 H$. Use the center dot to separate compound units, e.g., "A·m^2."

The word "data" is plural, not singular. The subscript for the permeability of vacuum μ_0 is zero, not a lowercase letter "o." The term for residual magnetization is "remanence"; the adjective is "remanent"; do not write "remnance" or "remnant." Use the word "micrometer" instead of "micron." A graph within a graph is an "inset," not an "insert." The word "alternatively" is preferred to the word "alternately" (unless you really mean something that alternates). Use the word "whereas" instead of "while" (unless you are referring to simultaneous events). Do not use the word "essentially" to mean "approximately" or "effectively." Do not use the word "issue" as a euphemism for "problem." When compositions are not specified, separate chemical symbols by en-dashes; for example, "NiMn" indicates the intermetallic compound $Ni_{0.5}Mn_{0.5}$ whereas "Ni–Mn" indicates an alloy of some composition Ni_xMn_{1-x}.

Be aware of the different meanings of the homophones "affect" (usually a verb) and "effect" (usually a noun), "complement" and "compliment," "discreet" and "discrete," "principal" (e.g., "principal investigator") and "principle" (e.g., "principle of measurement"). Do not confuse "imply" and "infer."

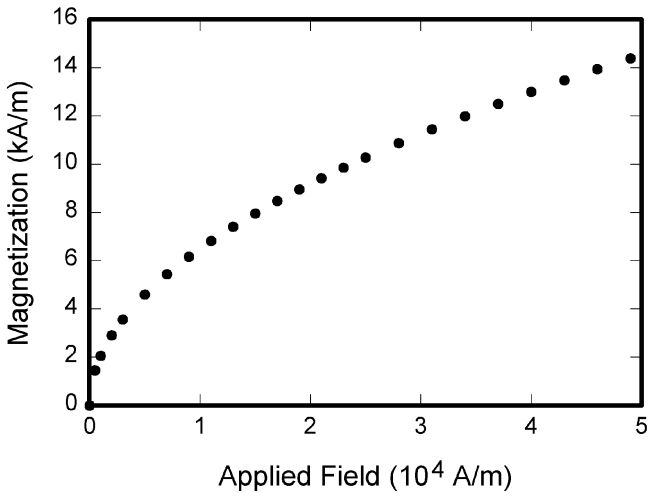

Fig. 11. Magnetization as a function of applied field. It is good practice to explain the significance of the figure in the caption.

Prefixes such as "non," "sub," "micro," "multi," and "ultra" are not independent words; they should be joined to the words they modify, usually without a hyphen. There is no period after the "et" in the Latin abbreviation "*et al.*" (it is also italicized). The abbreviation "i.e.," means "that is," and the abbreviation "e.g.," means "for example" (these abbreviations are not italicized).

A general IEEE styleguide is available at http://www.ieee.org/authortools.

VII. Guidelines for Graphics Preparation and Submission

A. Types of Graphics

The following list outlines the different types of graphics published in IEEE journals. They are categorized based on their construction, and use of color/shades of gray:

1) Color/Grayscale figures: Figures that are meant to appear in color, or shades of black/gray. Such figures may include photographs, illustrations, multicolor graphs, and flowcharts.

2) Line Art figures: Figures that are composed of only black lines and shapes. These figures should have no shades or halftones of gray, only black and white.

3) Author photos: Head and shoulders shots of authors that appear at the end of our papers.

4) Tables: Data charts which are typically black and white, but sometimes include color.

B. Multipart figures

Figures compiled of more than one sub-figure presented side-by-side, or stacked. If a multipart figure is made up of multiple figure types (one part is lineart, and another is grayscale or color) the figure should meet the stricter guidelines.

TABLE I
UNITS FOR MAGNETIC PROPERTIES

Symbol	Quantity	Conversion from Gaussian and CGS EMU to SI [a]
Φ	magnetic flux	1 Mx $\rightarrow 10^{-8}$ Wb $= 10^{-8}$ V·s
B	magnetic flux density, magnetic induction	1 G $\rightarrow 10^{-4}$ T $= 10^{-4}$ Wb/m^2
H	magnetic field strength	1 Oe $\rightarrow 10^3/(4\pi)$ A/m
m	magnetic moment	1 erg/G $=$ 1 emu $\rightarrow 10^{-3}$ A·m^2 $= 10^{-3}$ J/T
M	magnetization	1 erg/(G·cm^3) $=$ 1 emu/cm^3 $\rightarrow 10^3$ A/m
$4\pi M$	magnetization	1 G $\rightarrow 10^3/(4\pi)$ A/m
σ	specific magnetization	1 erg/(G·g) $=$ 1 emu/g $\rightarrow$ 1 A·m^2/kg
j	magnetic dipole moment	1 erg/G $=$ 1 emu $\rightarrow 4\pi \times 10^{-10}$ Wb·m
J	magnetic polarization	1 erg/(G·cm^3) $=$ 1 emu/cm^3 $\rightarrow 4\pi \times 10^{-4}$ T
χ, κ	susceptibility	1 $\rightarrow 4\pi$
χ_ρ	mass susceptibility	1 cm^3/g $\rightarrow 4\pi \times 10^{-3}$ m^3/kg
μ	permeability	1 $\rightarrow 4\pi \times 10^{-7}$ H/m $= 4\pi \times 10^{-7}$ Wb/(A·m)
μ_r	relative permeability	$\mu \rightarrow \mu_r$
w, W	energy density	1 erg/cm^3 $\rightarrow 10^{-1}$ J/m^3
N, D	demagnetizing factor	1 $\rightarrow 1/(4\pi)$

Vertical lines are optional in tables. Statements that serve as captions for the entire table do not need footnote letters.

[a]Gaussian units are the same as cg emu for magnetostatics; Mx = maxwell, G = gauss, Oe = oersted; Wb = weber, V = volt, s = second, T = tesla, m = meter, A = ampere, J = joule, kg = kilogram, H = henry.

C. File Formats For Graphics

Format and save your graphics using a suitable graphics processing program that will allow you to create the images as PostScript (PS), Encapsulated PostScript (.EPS), Tagged Image File Format (.TIFF), Portable Document Format (.PDF), Portable Network Graphics (.PNG), or Metapost (.MPS), sizes them, and adjusts the resolution settings. When submitting your final paper, your graphics should all be submitted individually in one of these formats along with the manuscript.

D. Sizing of Graphics

Most charts, graphs, and tables are one column wide (3.5 inches/88 millimeters/21 picas) or page wide (7.16 inches/181 millimeters/43 picas). The maximum depth a graphic can be is 8.5 inches (216 millimeters/54 picas). When choosing the depth of a graphic, please allow space for a caption. Figures can be sized between column and page widths if the author chooses, however it is recommended that figures are not sized less than column width unless when necessary.

There is currently one publication with column measurements that do not coincide with those listed above. Proceedings of the IEEE has a column measurement of 3.25 inches (82.5 millimeters/19.5 picas).

The final printed size of author photographs is exactly 1 inch wide by 1.25 inches tall (25.4 millimeters $\times$ 31.75 millimeters/6 picas $\times$ 7.5 picas). Author photos printed in editorials measure 1.59 inches wide by 2 inches tall (40 millimeters $\times$ 50 millimeters/9.5 picas $\times$ 12 picas).

E. Resolution

The proper resolution of your figures will depend on the type of figure it is as defined in the "Types of Figures" section. Author photographs, color, and grayscale figures should be at least 300dpi. Line art, including tables should be a minimum of 600dpi.

F. Vector Art

In order to preserve the figures' integrity across multiple computer platforms, we accept files in the following formats: .EPS/.PDF/.PS. All fonts must be embedded or text converted to outlines in order to achieve the best-quality results.

G. Color Space

The term color space refers to the entire sum of colors that can be represented within the said medium. For our purposes, the three main color spaces are Grayscale, RGB (red/green/blue) and CMYK (cyan/magenta/yellow/black). RGB is generally used with on-screen graphics, whereas CMYK is used for printing purposes.

All color figures should be generated in RGB or CMYK color space. Grayscale images should be submitted in Grayscale color space. Line art may be provided in grayscale OR bitmap colorspace. Note that "bitmap colorspace" and "bitmap file format" are not the same thing. When bitmap color space is selected, .TIF/.TIFF/.PNG are the recommended file formats.

H. Accepted Fonts Within Figures

When preparing your graphics IEEE suggests that you use of one of the following Open Type fonts: Times New Roman, Helvetica, Arial, Cambria, and Symbol. If you are supplying EPS, PS, or PDF files all fonts must be embedded. Some fonts may only be native to your operating system; without the fonts embedded, parts of the graphic may be distorted or missing.

A safe option when finalizing your figures is to strip out the fonts before you save the files, creating "outline" type. This converts fonts to artwork what will appear uniformly on any screen.

I. Using Labels Within Figures

1) Figure Axis labels : Figure axis labels are often a source of confusion. Use words rather than symbols. As an example, write the quantity "Magnetization," or "Magnetization M," not just "M." Put units in parentheses. Do not label axes only with units. As in Fig. 1, for example, write "Magnetization (A/m)" or "Magnetization (A·m^{-1})," not just "A/m." Do not label axes with a ratio of quantities and units. For example, write "Temperature (K)," not "Temperature/K."

Multipliers can be especially confusing. Write "Magnetization (kA/m)" or "Magnetization (10^3 A/m)." Do not write "Magnetization (A/m) $\times$ 1000" because the reader would not know whether the top axis label in Fig. 1 meant 16000 A/m or 0.016 A/m. Figure labels should be legible, approximately 8 to 10 point type.

2) Subfigure Labels in Multipart Figures and Tables: Multipart figures should be combined and labeled before final submission.

Labels should appear centered below each subfigure in 8 point Times New Roman font in the format of (a) (b) (c).

J. File Naming

Figures (line artwork or photographs) should be named starting with the first 5 letters of the author's last name. The next characters in the filename should be the number that represents the sequential location of this image in your article. For example, in author "Anderson's" paper, the first three figures would be named ander1.tif, ander2.tif, and ander3.ps.

Tables should contain only the body of the table (not the caption) and should be named similarly to figures, except that '.t' is inserted in-between the author's name and the table number. For example, author Anderson's first three tables would be named ander.t1.tif, ander.t2.ps, ander.t3.eps.

Author photographs should be named using the first five characters of the pictured author's last name. For example, four author photographs for a paper may be named: oppen.ps, moshc.tif, chen.eps, and duran.pdf.

If two authors or more have the same last name, their first initial(s) can be substituted for the fifth, fourth, third. . . letters of their surname until the degree where there is differentiation. For example, two authors Michael and Monica Oppenheimer's photos would be named oppmi.tif, and oppmo.eps.

K. Referencing a Figure or Table Within Your Paper

When referencing your figures and tables within your paper, use the abbreviation "Fig." even at the beginning of a sentence. Do not abbreviate "Table." Tables should be numbered with Roman Numerals.

L. Checking Your Figures: The IEEE Graphics Analyzer

The IEEE Graphics Analyzer enables authors to pre-screen their graphics for compliance with IEEE Transactions and Journals standards before submission.

The online tool, located at http://graphicsqc.ieee.org/, allows authors to upload their graphics in order to check that each file is the correct file format, resolution, size and colorspace; that no fonts are missing or corrupt; that figures are not compiled in layers or have transparency, and that they are named according to the IEEE Transactions and Journals naming convention. At the end of this automated process, authors are provided with a detailed report on each graphic within the web applet, as well as by email.

For more information on using the Graphics Analyzer or any other graphics related topic, contact the IEEE Graphics Help Desk by e-mail at graphics@ieee.org.

M. Submitting Your Graphics

Because IEEE will do the final formatting of your paper, you do not need to position figures and tables at the top and bottom of each column. In fact, all figures, figure captions, and tables can be placed at the end of your paper. In addition to, or even in lieu of submitting figures within your final manuscript, figures should be submitted individually, separate from the manuscript in one of the file formats listed above in Section VII-C. Place figure captions below the figures; place table titles above the tables. Please do not include captions as part of the figures, or put them in "text boxes" linked to the figures. Also, do not place borders around the outside of your figures.

N. Color Processing/Printing in IEEE Journals

All IEEE Transactions, Journals, and Letters allow an author to publish color figures on IEEE Xplore® at no charge, and automatically convert them to grayscale for print versions. In most journals, figures and tables may alternatively be printed in color if an author chooses to do so.

Please note that this service comes at an extra expense to the author. If you intend to have print color graphics, include a note with your final paper indicating which figures or tables you would like to be handled that way, and stating that you are willing to pay the additional fee.

VIII. Conclusion

A conclusion section is not required. Although a conclusion may review the main points of the paper, do not replicate the abstract as the conclusion. A conclusion might elaborate on the importance of the work or suggest applications and extensions.

Appendixes, if needed, appear before the acknowledgment.

Acknowledgment

The preferred spelling of the word "acknowledgment" in American English is without an "e" after the "g." Use the singular heading even if you have many acknowledgments. Avoid expressions such as "One of us (S.B.A.) would like to thank . . . ." Instead, write "F. A. Author thanks . . . ." In most cases, sponsor and financial support acknowledgments are placed in the unnumbered footnote on the first page, not here.

References and Footnotes

A. References

References need not be cited in text. When they are, they appear on the line, in square brackets, inside the punctuation. Multiple references are each numbered with separate brackets. When citing a section in a book, please give the relevant page numbers. In text, refer simply to the reference number. Do not use "Ref." or "reference" except at the beginning of a sentence: "Reference [3] shows . . . ." Please do not use automatic endnotes in *Word*, rather, type the reference list at the end of the paper using the "References" style.

Reference numbers are set flush left and form a column of their own, hanging out beyond the body of the reference. The reference numbers are on the line, enclosed in square brackets. In all references, the given name of the author or editor is abbreviated to the initial only and precedes the last name. Use them all; use *et al.* only if names are not given. Use commas around Jr., Sr., and III in names. Abbreviate conference titles. When citing IEEE transactions, provide the

issue number, page range, volume number, year, and/or month if available. When referencing a patent, provide the day and the month of issue, or application. References may not include all information; please obtain and include relevant information. Do not combine references. There must be only one reference with each number. If there is a URL included with the print reference, it can be included at the end of the reference.

Other than books, capitalize only the first word in a paper title, except for proper nouns and element symbols. For papers published in translation journals, please give the English citation first, followed by the original foreign-language citation See the end of this document for formats and examples of common references. For a complete discussion of references and their formats, see the IEEE style manual at http://www.ieee.org/authortools.

B. Footnotes

Number footnotes separately in superscript numbers.[1] Place the actual footnote at the bottom of the column in which it is cited; do not put footnotes in the reference list (endnotes). Use letters for table footnotes (see Table I).

Appendix I
Submitting Your Paper for Review

A. Final Stage

When you submit your final version (after your paper has been accepted), print it in two-column format, including figures and tables. You must also send your final manuscript on a disk, via e-mail, or through a Web manuscript submission system as directed by the society contact. You may use *Zip* for large files, or compress files using *Compress, Pkzip, Stuffit,* or *Gzip*.

Also, send a sheet of paper or PDF with complete contact information for all authors. Include full mailing addresses, telephone numbers, fax numbers, and e-mail addresses. This information will be used to send each author a complimentary copy of the journal in which the paper appears. In addition, designate one author as the "corresponding author." This is the author to whom proofs of the paper will be sent. Proofs are sent to the corresponding author only.

B. Review Stage Using ScholarOne® Manuscripts

Contributions to the Transactions, Journals, and Letters may be submitted electronically on IEEE's online manuscript submission and peer-review system, ScholarOne® Manuscripts. You can get a listing of the publications that participate in ScholarOne at http://www.ieee.org/publications_standards/publications/authors/authors_submission.html. First check if you have an existing account. If there is none, please create a new account. After logging in, go to your Author Center and click "Submit First Draft of a New Manuscript."

[1]It is recommended that footnotes be avoided (except for the unnumbered footnote with the receipt date on the first page). Instead, try to integrate the footnote information into the text.

Along with other information, you will be asked to select the subject from a pull-down list. Depending on the journal, there are various steps to the submission process; you must complete all steps for a complete submission.

At the end of each step you must click "Save and Continue"; just uploading the paper is not sufficient. After the last step, you should see a confirmation that the submission is complete. You should also receive an e-mail confirmation. For inquiries regarding the submission of your paper on ScholarOne Manuscripts, please contact oprs-support@ieee.org or call +1 732 465 5861.

ScholarOne Manuscripts will accept files for review in various formats.

Please check the guidelines of the specific journal for which you plan to submit.

You will be asked to file an electronic copyright form immediately upon completing the submission process (authors are responsible for obtaining any security clearances). Failure to submit the electronic copyright could result in publishing delays later. You will also have the opportunity to designate your article as "open access" if you agree to pay the IEEE open access fee.

C. Final Stage Using ScholarOne Manuscripts

Upon acceptance, you will receive an email with specific instructions regarding the submission of your final files. To avoid any delays in publication, please be sure to follow these instructions. Most journals require that final submissions be uploaded through ScholarOne Manuscripts, although some may still accept final submissions via email. Final submissions should include source files of your accepted manuscript, high quality graphic files, and a formatted pdf file. If you have any questions regarding the final submission process, please contact the administrative contact for the journal.

In addition to this, upload a file with complete contact information for all authors. Include full mailing addresses, telephone numbers, fax numbers, and e-mail addresses. Designate the author who submitted the manuscript on ScholarOne Manuscripts as the "corresponding author." This is the only author to whom proofs of the paper will be sent.

D. Copyright Form

Authors must submit an electronic IEEE Copyright Form (eCF) upon submitting their final manuscript files. You can access the eCF system through your manuscript submission system or through the Author Gateway. You are responsible for obtaining any necessary approvals and/or security clearances. For additional information on intellectual property rights, visit the IEEE Intellectual Property Rights department web page at http://www.ieee.org/publications_standards/publications/rights/index.html.

Appendix II
IEEE Publishing Policy

The general IEEE policy requires that authors should only submit original work that has neither appeared elsewhere

for publication, nor is under review for another refereed publication. The submitting author must disclose all prior publication(s) and current submissions when submitting a manuscript. Do not publish "preliminary" data or results. The submitting author is responsible for obtaining agreement of all coauthors and any consent required from employers or sponsors before submitting an article.

The IEEE Transactions and Journals Department strongly discourages courtesy authorship; it is the obligation of the authors to cite only relevant prior work.

The IEEE Transactions and Journals Department does not publish conference records or proceedings, but can publish articles related to conferences that have undergone rigorous peer review. Minimally, two reviews are required for every article submitted for peer review.

APPENDIX III
PUBLICATION PRINCIPLES

The two types of contents of that are published are; 1) peer-reviewed and 2) archival. The Transactions and Journals Department publishes scholarly articles of archival value as well as tutorial expositions and critical reviews of classical subjects and topics of current interest.

Authors should consider the following points:

1) Technical papers submitted for publication must advance the state of knowledge and must cite relevant prior work.
2) The length of a submitted paper should be commensurate with the importance, or appropriate to the complexity, of the work. For example, an obvious extension of previously published work might not be appropriate for publication or might be adequately treated in just a few pages.
3) Authors must convince both peer reviewers and the editors of the scientific and technical merit of a paper; the standards of proof are higher when extraordinary or unexpected results are reported.
4) Because replication is required for scientific progress, papers submitted for publication must provide sufficient information to allow readers to perform similar experiments or calculations and use the reported results. Although not everything need be disclosed, a paper must contain new, useable, and fully described information. For example, a specimen's chemical composition need not be reported if the main purpose of a paper is to introduce a new measurement technique. Authors should expect to be challenged by reviewers if the results are not supported by adequate data and critical details.
5) Papers that describe ongoing work or announce the latest technical achievement, which are suitable for presentation at a professional conference, may not be appropriate for publication.

APPENDIX IV
REFERENCE EXAMPLES

- *Basic format for books:*
  J. K. Author, "Title of chapter in the book," in *Title of His Published Book, x*th ed. City of Publisher, (only U.S. State), Country: Abbrev. of Publisher, year, ch. x, sec. x, pp. *xxx–xxx.*
  See [1], [2].
- *Basic format for periodicals:*
  J. K. Author, "Name of paper," *Abbrev. Title of Periodical*, vol. *x, no*. x,pp. *xxx–xxx,* Abbrev. Month, year, DOI. 10.1109.*XXX*.123456.
  See [3]– [5].
- *Basic format for reports:*
  J. K. Author, "Title of report," Abbrev. Name of Co., City of Co., Abbrev. State, Country, Rep. *xxx*, year.
  See [6], [7].
- *Basic format for handbooks:*
  Name of Manual/Handbook, x ed., Abbrev. Name of Co., City of Co., Abbrev. State, Country, year, pp. *xxx–xxx.*
  See [8], [9].
- *Basic format for books (when available online):*
  J. K. Author, "Title of chapter in the book," in *Title of Published Book*, xth ed. City of Publisher, State, Country: Abbrev. of Publisher, year, ch. x, sec. x, pp. *xxx–xxx*. [Online]. Available: http://www.web.com
  See [10]– [13].
- *Basic format for journals (when available online):*
  J. K. Author, "Name of paper," *Abbrev. Title of Periodical*, vol. x, no. x, pp. *xxx–xxx*, Abbrev. Month, year. Accessed on: Month, Day, year, DOI: 10.1109.*XXX*.123456, [Online].
  See [14]– [16].
- *Basic format for papers presented at conferences (when available online):*
  J.K. Author. (year, month). Title. presented at abbrev. conference title. [Type of Medium]. Available: site/path/file
  See [17].
- *Basic format for reports and handbooks (when available online):*
  J. K. Author. "Title of report," Company. City, State, Country. Rep. no., (optional: vol./issue), Date. [Online] Available: site/path/file
  See [18], [19].
- *Basic format for computer programs and electronic documents (when available online):*
  Legislative body. Number of Congress, Session. (year, month day). *Number of bill or resolution*, *Title*. [Type of medium]. Available: site/path/file
  NOTE: **ISO recommends that capitalization follow the accepted practice for the language or script in which the information is given.**
  See [20].
- *Basic format for patents (when available online):*
  Name of the invention, by inventor's name. (year, month day). Patent Number [Type of medium]. Available: site/path/file
  See [21].
- *Basic formatfor conference proceedings (published):*
  J. K. Author, "Title of paper," in *Abbreviated Name of Conf.*, City of Conf., Abbrev. State (if given), Country, year, pp. *xxxxxx.*

See [22].

- *Example for papers presented at conferences (unpublished):*
  See [23].
- *Basic format for patents*:
  J. K. Author, "Title of patent," U.S. Patent *x xxx xxx*, Abbrev. Month, day, year.
  See [24].
- *Basic format for theses (M.S.) and dissertations (Ph.D.):*
  1) J. K. Author, "Title of thesis," M.S. thesis, Abbrev. Dept., Abbrev. Univ., City of Univ., Abbrev. State, year.
  2) J. K. Author, "Title of dissertation," Ph.D. dissertation, Abbrev. Dept., Abbrev. Univ., City of Univ., Abbrev. State, year.

  See [25], [26].
- *Basic format for the most common types of unpublished references:*
  1) J. K. Author, private communication, Abbrev. Month, year.
  2) J. K. Author, "Title of paper," unpublished.
  3) J. K. Author, "Title of paper," to be published.

  See [27]– [29].
- *Basic formats for standards:*
  1) *Title of Standard*, Standard number, date.
  2) *Title of Standard*, Standard number, Corporate author, location, date.

  See [30], [31].
- *Article number in reference examples:*
  See [32], [33].
- *Example when using et al.:*
  See [34].

REFERENCES

[1] G. O. Young, "Synthetic structure of industrial plastics," in *Plastics,* 2nd ed., vol. 3, J. Peters, Ed. New York, NY, USA: McGraw-Hill, 1964, pp. 15–64.

[2] W.-K. Chen, *Linear Networks and Systems.* Belmont, CA, USA: Wadsworth, 1993, pp. 123–135.

[3] J. U. Duncombe, "Infrared navigation—Part I: An assessment of feasibility," *IEEE Trans. Electron Devices*, vol. ED-11, no. 1, pp. 34–39, Jan. 1959, 10.1109/TED.2016.2628402.

[4] E. P. Wigner, "Theory of traveling-wave optical laser," *Phys. Rev*., vol. 134, pp. A635–A646, Dec. 1965.

[5] E. H. Miller, "A note on reflector arrays," *IEEE Trans. Antennas Propagat*., to be published.

[6] E. E. Reber, R. L. Michell, and C. J. Carter, "Oxygen absorption in the earth's atmosphere," Aerospace Corp., Los Angeles, CA, USA, Tech. Rep. TR-0200 (4230-46)-3, Nov. 1988.

[7] J. H. Davis and J. R. Cogdell, "Calibration program for the 16-foot antenna," Elect. Eng. Res. Lab., Univ. Texas, Austin, TX, USA, Tech. Memo. NGL-006-69-3, Nov. 15, 1987.

[8] *Transmission Systems for Communications*, 3rd ed., Western Electric Co., Winston-Salem, NC, USA, 1985, pp. 44–60.

[9] *Motorola Semiconductor Data Manual*, Motorola Semiconductor Products Inc., Phoenix, AZ, USA, 1989.

[10] G. O. Young, "Synthetic structure of industrial plastics," in Plastics, vol. 3, Polymers of Hexadromicon, J. Peters, Ed., 2nd ed. New York, NY, USA: McGraw-Hill, 1964, pp. 15-64. [Online]. Available: http://www.bookref.com.

[11] *The Founders' Constitution*, Philip B. Kurland and Ralph Lerner, eds., Chicago, IL, USA: Univ. Chicago Press, 1987. [Online]. Available: http://press-pubs.uchicago.edu/founders/

[12] The Terahertz Wave eBook. ZOmega Terahertz Corp., 2014. [Online]. Available: http://dl.z-thz.com/eBook/zomega_ebook_pdf_1206_sr.pdf. Accessed on: May 19, 2014.

[13] Philip B. Kurland and Ralph Lerner, eds., *The Founders' Constitution.* Chicago, IL, USA: Univ. of Chicago Press, 1987, Accessed on: Feb. 28, 2010, [Online] Available: http://press-pubs.uchicago.edu/founders/

[14] J. S. Turner, "New directions in communications," *IEEE J. Sel. Areas Commun*., vol. 13, no. 1, pp. 11-23, Jan. 1995.

[15] W. P. Risk, G. S. Kino, and H. J. Shaw, "Fiber-optic frequency shifter using a surface acoustic wave incident at an oblique angle," *Opt. Lett.*, vol. 11, no. 2, pp. 115–117, Feb. 1986.

[16] P. Kopyt *et al.,* "Electric properties of graphene-based conductive layers from DC up to terahertz range," *IEEE THz Sci. Technol.,* to be published. DOI: 10.1109/TTHZ.2016.2544142.

[17] PROCESS Corporation, Boston, MA, USA. Intranets: Internet technologies deployed behind the firewall for corporate productivity. Presented at INET96 Annual Meeting. [Online]. Available: http://home.process.com/Intranets/wp2.htp

[18] R. J. Hijmans and J. van Etten, "Raster: Geographic analysis and modeling with raster data," R Package Version 2.0-12, Jan. 12, 2012. [Online]. Available: http://CRAN.R-project.org/package=raster

[19] Teralyzer. Lytera UG, Kirchhain, Germany [Online]. Available: http://www.lytera.de/Terahertz_THz_Spectroscopy.php?id=home, Accessed on: Jun. 5, 2014

[20] U.S. House. 102nd Congress, 1st Session. (1991, Jan. 11). *H. Con. Res. 1, Sense of the Congress on Approval of Military Action*. [Online]. Available: LEXIS Library: GENFED File: BILLS

[21] Musical toothbrush with mirror, by L.M.R. Brooks. (1992, May 19). Patent D 326 189 [Online]. Available: NEXIS Library: LEXPAT File: DES

[22] D. B. Payne and J. R. Stern, "Wavelength-switched pas- sively coupled single-mode optical network," in *Proc. IOOC-ECOC,* Boston, MA, USA, 1985, pp. 585–590.

[23] D. Ebehard and E. Voges, "Digital single sideband detection for interferometric sensors," presented at the *2nd Int. Conf. Optical Fiber Sensors,* Stuttgart, Germany, Jan. 2-5, 1984.

[24] G. Brandli and M. Dick, "Alternating current fed power supply," U.S. Patent 4 084 217, Nov. 4, 1978.

[25] J. O. Williams, "Narrow-band analyzer," Ph.D. dissertation, Dept. Elect. Eng., Harvard Univ., Cambridge, MA, USA, 1993.

[26] N. Kawasaki, "Parametric study of thermal and chemical nonequilibrium nozzle flow," M.S. thesis, Dept. Electron. Eng., Osaka Univ., Osaka, Japan, 1993.

[27] A. Harrison, private communication, May 1995.

[28] B. Smith, "An approach to graphs of linear forms," unpublished.

[29] A. Brahms, "Representation error for real numbers in binary computer arithmetic," IEEE Computer Group Repository, Paper R-67-85.

[30] IEEE Criteria for Class IE Electric Systems, IEEE Standard 308, 1969.

[31] Letter Symbols for Quantities, ANSI Standard Y10.5-1968.

[32] R. Fardel, M. Nagel, F. Nuesch, T. Lippert, and A. Wokaun, "Fabrication of organic light emitting diode pixels by laser-assisted forward transfer," *Appl. Phys. Lett.*, vol. 91, no. 6, Aug. 2007, Art. no. 061103.

[33] J. Zhang and N. Tansu, "Optical gain and laser characteristics of InGaN quantum wells on ternary InGaN substrates," *IEEE Photon. J.*, vol. 5, no. 2, Apr. 2013, Art. no. 2600111

[34] S. Azodolmolky *et al.*, Experimental demonstration of an impairment aware network planning and operation tool for transparent/translucent optical networks," *J. Lightw. Technol.*, vol. 29, no. 4, pp. 439–448, Sep. 2011.

First A. Author (M'76–SM'81–F'87) and all authors may include biographies. Biographies are often not included in conference-related papers. This author became a Member (M) of IEEE in 1976, a Senior Member (SM) in 1981, and a Fellow (F) in 1987. The first paragraph may contain a place and/or date of birth (list place, then date). Next, the author's educational background is listed. The degrees should be listed with type of degree in what field, which institution, city, state, and country, and year the degree was earned. The author's major field of study should be lower-cased.

The second paragraph uses the pronoun of the person (he or she) and not the author's last name. It lists military and work experience, including summer and fellowship jobs. Job titles are capitalized. The current job must have a location; previous positions may be listed without one. Information concerning previous publications may be included.

Try not to list more than three books or published articles. The format for listing publishers of a book within the biography is: title of book (publisher name, year) similar to a reference. Current and previous research interests end the paragraph. The third paragraph begins with the author's title and last name (e.g., Dr. Smith, Prof. Jones, Mr. Kajor, Ms. Hunter).

List any memberships in professional societies other than the IEEE. Finally, list any awards and work for IEEE committees and publications. If a photograph is provided, it should be of good quality, and professional-looking. Following are two examples of an author's biography.

Second B. Author was born in Greenwich Village, New York, NY, USA in 1977. He received the B.S. and M.S. degrees in aerospace engineering from the University of Virginia, Charlottesville, in 2001 and the Ph.D. degree in mechanical engineering from Drexel University, Philadelphia, PA, in 2008.

From 2001 to 2004, he was a Research Assistant with the Princeton Plasma Physics Laboratory. Since 2009, he has been an Assistant Professor with the Mechanical Engineering Department, Texas A&M University, College Station.

He is the author of three books, more than 150 articles, and more than 70 inventions. His research interests include high-pressure and high-density nonthermal plasma discharge processes and applications, microscale plasma discharges, discharges in liquids, spectroscopic diagnostics, plasma propulsion, and innovation plasma applications. He is an Associate Editor of the journal *Earth, Moon, Planets*, and holds two patents.

Dr. Author was a recipient of the International Association of Geomagnetism and Aeronomy Young Scientist Award for Excellence in 2008, and the IEEE Electromagnetic Compatibility Society Best Symposium Paper Award in 2011.

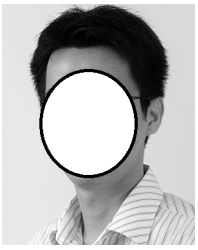

Third C. Author, Jr. (M'87) received the B.S. degree in mechanical engineering from National Chung Cheng University, Chiayi, Taiwan, in 2004 and the M.S. degree in mechanical engineering from National Tsing Hua University, Hsinchu, Taiwan, in 2006. He is currently pursuing the Ph.D.

degree in mechanical engineering at Texas A&M University, College Station, TX, USA.

From 2008 to 2009, he was a Research Assistant with the Institute of Physics, Academia Sinica, Tapei, Taiwan. His research interest includes the development of surface processing and biological/medical treatment techniques using nonthermal atmospheric pressure plasmas, fundamental study of plasma sources, and fabrication of micro- or nanostructured surfaces.

Mr. Author's awards and honors include the Frew Fellowship (Australian Academy of Science), the I. I. Rabi Prize (APS), the European Frequency and Time Forum Award, the Carl Zeiss Research Award, the William F. Meggers Award and the Adolph Lomb Medal (OSA).